Critical currents in the anisotropic superconductor $2H$-$NbSe_2$: Evidence for an upper bound of the surface critical-current density

G. Lazard, P. Mathieu, B. Plaçais, J. Mosqueira,* and Y. Simon
Laboratoire de Physique de la Matière Condensée de l'Ecole Normale Supérieure, F-75231 Paris Cedex 05, France

C. Guilpin
Groupe de Physique des Solides, F-75251 Paris Cedex 05, France

G. Vacquier
MADIREL, Centre Saint Charles, Université de Provence, 13331 Marseille Cedex 03, France
(Received 11 July 2001; published 22 January 2002)

According to the Mathieu-Simon continuum theory of the vortex state, a large nondissipative supercurrent can flow over a small depth from a rough surface, up to an easily estimated critical value K_c(A/m) of the surface current density. It is shown that K_c must saturate at high fields in an anisotropic crystal when the surface roughness is increased, and the corresponding upper bound only depends on fundamental parameters of the material. Measurements in $2H$-$NbSe_2$ crystals confirm this saturation effect quantitatively, as well as the proposed idea that, in a large class of soft samples, the critical current should be entirely accounted for by surface K_c currents.

DOI: 10.1103/PhysRevB.65.064518 PACS number(s): 74.60.Jg, 74.20.De, 74.70.Ad

I. INTRODUCTION

Some years ago, Mathieu and Simon (MS) developed a continuum theory of the mixed state.[1,2] The MS theory shedded light on dc and ac transport properties of type-II superconductors. Basic questions have been reexamined, beginning with the mere equilibrium of a perfect body (see Fig. 2 of Ref. 2), where diamagnetic currents are treated on the same footing as nondissipative transport currents.[2] Further intricate and unsolved problems involving flux flow and dissipation have been explained successfully, as, for example, the mechanism of flux-flow noise,[3] and the frequency dependence of the surface impedance across the so-called depinning transition.[4] Furthermore, surprising effects can be predicted such as those discussed in this paper.

The MS theory has given rise to some controversy about the location of critical currents, as well as the underlying physics. In this paper we present additional arguments, both experimental and theoretical, concerning the very nature of critical currents. Postponing theoretical details (Sec. II), let us first point out some qualitative conclusions of the MS model for critical currents.

A sample where all thermodynamic local parameters would be slowly varying functions of position, and the surface of which would be smooth on the scale of the vortex distance, could be regarded as perfect with zero hysteresis or critical currents. Of course, such an ideal sample cannot exist, merely because any surface exhibits unavoidable irregularities on a scale comparable to or smaller than the vortex spacing. Attention should be paid to these kinds of defects. In fact, the surface roughness introduces disorder in the boundary conditions, giving rise to many possible metastable states of equilibrium corresponding to many ways for vortices to terminate at the sample surface.[1,2] Now, according to the MS equations for vortex equilibrium [Eqs. (4) and (5) below], this circumstance just causes the ability of the surface to carry nondissipative surface currents K (A/m) distributed over a small depth $\lambda_V \leqslant \lambda$ (the London penetration depth).[2,5] The limiting value K_c of the surface current density in general increases with increasing roughness. Then, the chief point is that expected values of K_c fully account for both the order of magnitude and the field and temperature dependence of critical currents, such as those observed in a large class of soft samples. We naturally exclude the case of (hard) samples crossed by interfaces or large bulk inhomogeneities, which can transport bulk nondissipative currents (multifilaments in industrial wires, twin boundaries in a YBaCuO (YBCO) crystal, sintered powders, etc).

Critical-current densities associated in this way with the surface roughness are readily estimated, so that one may at least infer that K_c currents represent in any case a large contribution to the whole critical current. Moreover, as discussed in previous papers,[1–4] there are experimental grounds for believing that critical currents in many standard samples, including $NbSe_2$ crystals used in this work, are nothing but MS superficial currents K_c. In such samples, any deviation of the ideal electromagnetic response should be entirely governed by the state of the surface.

In this respect, recent measurements of the surface impedance in thick slabs of conventional materials, either polycrystals or single crystals (PbIn, Nb, and V), are particularly convincing.[4] The detailed frequency spectrum of the linear ac response has been quantitatively explained by a two-modes skin effect in accordance with the MS theory. The excellent agreement between experiment and theory proves that bulk vortices do respond freely; the least bulk pinning would affect the penetrating mode significantly, and could not escape notice.[4]

Another naive observation may provide a clue, although it is not a conclusive argument. Critical currents are generally expressed in terms of critical-current densities J_c (A/m^2), taking for granted that nondissipative transport currents are

uniformly distributed over the cross section. However, when data are taken in a series of films or foils of variable thickness t, J_c (defined as I_c/Wt, where W is the foil width) is generally observed to increase with decreasing t. More precisely, Joiner and Kuhl[6] reported an exact linear dependence J_c vs $1/t$ in PbBi foils. A similar behavior is retrieved in YBCO films, when the thickness is larger than about $2\lambda_{ab}$,[7] for example, $J_c t \sim 10$ A/cm in the low-field limit at 70 K.[8] The fact that $J_c t = \text{const}$ in samples otherwise prepared in the same way could be immediately and most simply interpreted by stating that $K_c = I_c/2W = \text{const}$.

The following objection has been raised. While nobody denies that surface pinning may play an important role, the idea that in the same sample bulk pinning could be ineffective offends common sense. In this connection, we stress that the ability of the surface to carry a nondissipative transport current owing to the disorder of the boundary conditions *is not* a mechanism of pinning in the proper sense. It is not the effect of local variations of the free energy in the vicinity of pinning centers that causes some locations of a vortex to be favored over others. So the goal here is not to compare the relative weight of surface to bulk pinning, but to know whether the MS currents K_c do or do not provide an alternative relevant mechanism. It should also be noted that we are unable to get pinning parameters of an actual sample, such as the density of pins and the magnitude of the pinning force, allowing us to calculate related values of J_c to be compared with experiment. Therefore, no quantitative estimate can decide for or against the importance of bulk pinning. On the contrary, in the exceptional case of strongly roughened surfaces of anisotropic crystals, absolute values of K_c can be calculated exactly as a function of well-known parameters. We thus expect the comparison in this case between theoretical K_c and measured I_c to be very instructive.

II. THEORY OF THE CRITICAL-CURRENT DENSITY K_c IN AN ANISOTROPIC SUPERCONDUCTOR

A. The continuum equations for vortex equilibrium

In this section, we briefly recall the basic MS equations with regard only to nondissipative states. The mean free-energy density of a vortex continuum can be expressed in terms of a reduced set of macroscopic variables; ''macroscopic'' here means averaged on a scale larger than the vortex spacing. Then, the macroscopic thermodynamic identity, such as that derived by averaging the Ginzburg-Landau (GL) free energy, reads[2,9]

$$d\overline{F} = -\sigma dT + \frac{1}{\mu_0}\mathbf{B}\cdot d\mathbf{B} - \frac{m}{e}\mathbf{J_s}\cdot d\mathbf{V_s} + \boldsymbol{\varepsilon}\cdot d\boldsymbol{\omega}. \qquad (1)$$

$\mathbf{B} = \overline{\mathbf{b}}$, $\mathbf{J_s} = \overline{\mathbf{j_s}}$, and $\mathbf{V_s} = \overline{\mathbf{v_s}}$ are the macroscopic magnetic field, supercurrent density, and velocity, respectively. The vortex field $\boldsymbol{\omega} = n\varphi_0\boldsymbol{\nu}$ describes both the local density n and direction $\boldsymbol{\nu}$ of the vortex array (φ_0 is the flux quantum). Two simple results have come out: $\partial\overline{F}/\partial\mathbf{B} = \mathbf{B}/\mu_0$, and $\mathbf{J_s}$ is the conjugate variable of $\mathbf{V_s}$. Otherwise, explicit calculations and/or approximations are required to obtain the fundamental equations of state $\mathbf{J_s}(T, \boldsymbol{\omega}, \mathbf{V_s})$ and $\boldsymbol{\varepsilon}(T, \boldsymbol{\omega}, \mathbf{V_s})$.

One essential point in the MS formalism is the imperative distinction to be made from the outset between $\boldsymbol{\omega}$ and $\mathbf{B}$. On multiplying $n\boldsymbol{\nu}$ by φ_0, $\boldsymbol{\omega}$ and $\boldsymbol{\varepsilon}$, defined as $\partial\overline{F}/\partial\boldsymbol{\omega}$, have been conveniently but artificially expressed in tesla and A/m, respectively (rationalized units). Yet the expression ''vortex induction'' for $\boldsymbol{\omega}$, sometimes used in the literature, is misleading. Local vortex currents $\mathbf{j_s}$, whether $\mathbf{J_s} = 0$ or not, do not contribute to the local macroscopic magnetic field $\mathbf{B}$. Irrespective of the local vortex ordering, the field $\mathbf{B}$ at a given point is set up by currents $\mathbf{J_s}$ flowing everywhere else in the sample, and also as by external currents $\mathbf{J}_0$ (sources of the applied field $\mathbf{B}_0$). Therefore, one may expect that, at some points, $\boldsymbol{\omega}$ and $\mathbf{B}$ have different values; in other words, there may be regions where magnetic-field lines do not coincide with vortex lines.

By using only the parameter $\boldsymbol{\omega}$ to describe the vortex lattice, MS theory deliberately disregards very small differences in energy associated with distortions of the unit cell and related shear stresses. Consequently, the MS interpretation of the critical currents will hold for a ''vortex liquid'' as well. This is a marked difference with classical theories of pinning where the shear elastic constant c_{66}, however small, plays a leading part.

The second and third terms in Eq. (1) stand for the macroscopic magnetic and kinetic energies. At high fields (say, $B \geqslant 0.5B_{c2}$), $\mathbf{B}^2/2\mu_0$ represents typically more than 90% of the free-energy density. The last term derives from small positive corrections in the free energy arising from ''microscopic'' oscillations of fields on the scale of the vortex spacing (on averaging quadratic terms $\overline{\mathbf{b}^2} > \mathbf{B}^2$, etc.). Although $\mathbf{B}$, $\boldsymbol{\omega}$, and $\mathbf{V_s}$ (or $\mathbf{J_s}$) must be regarded locally as three independent thermodynamic variables, it remains that their spatial variations are subject to constraints, viz, Ampere's law and the macroscopic London equation:

$$\text{curl}\,\mathbf{B} = \mu_0\mathbf{J_s}, \qquad (2)$$

$$\mathbf{B} - \frac{m}{e}\text{curl}\,\mathbf{V_s} = \boldsymbol{\omega}. \qquad (3)$$

Equation (3) follows from a proper average of curl $\mathbf{p_s}$ (the momentum of the supercurrent):[2] curl $\mathbf{p_s} = 0$ everywhere except on the vortex lines, and the line integral of $\mathbf{p_s}$ around a closed path encircling N vortices is Nh. It reduces to the usual London equation in the absence of vortices ($\boldsymbol{\omega} = 0$). In regions where the vortex lattice is perfectly regular, there are no macroscopic currents ($\mathbf{J_s} \equiv 0$ and $\mathbf{V_s} \equiv 0$), and Eq. (3) reduces to the familiar equality $\boldsymbol{\omega} = \mathbf{B}$ ($B = n\varphi_0$).

Minimizing the magnetic free enthalpy against small variations of $\mathbf{B}$, $\mathbf{J_s}$, and $\boldsymbol{\omega}$, subject to constraints (2) and (3), leads to the following equilibrium conditions, which also govern nondissipative states:[2]

$$\mathbf{J_s} + \text{curl}\,\boldsymbol{\varepsilon} = 0, \qquad (4)$$

$$\boldsymbol{\varepsilon} \times \mathbf{n} = 0, \qquad (5)$$

where $\mathbf{n}$ is the outward normal unit vector at the sample surface. As required by a continuum description, in deriving

Eq. (5), the surface has been supposed to be ideal, that is, smooth on the scale of a few vortex spacings. We shall return later to rough surfaces.

In the *isotropic* case, for instance, $\boldsymbol{\varepsilon}$ is directed along vortices, and Eq. (5) states that vortex lines must terminate perpendicular to the sample surface. This is consistent with the ''microscopic'' GL boundary condition $\partial\rho/\partial n=0$ for the order parameter Ψ ($\rho=|\Psi|$), which requires a vortex core line $\Psi=0$ to end normal to the surface. Taking the cross product of Eq. (4) with $\varphi_0\boldsymbol{\nu}$, this may be read as the balance of a Lorentz force, $\mathbf{J_s}\times\varphi_0\boldsymbol{\nu}$ and a restoring force, curl $\varepsilon\times\varphi_0\boldsymbol{\nu}$, resulting from vortex curvature with a line tension $\boldsymbol{\varepsilon}\varphi_0$.

The equilibrium of a simple *perfect* body (sphere, cylinder, slab, etc.) of rather large size, immersed in an external field $\mathbf{B}_0$, is determined by the above set of Eqs. (2)–(5).[2] Vortices are uniformly distributed in the bulk ($\boldsymbol{\omega}_1=\mathbf{B}_1=$const), but they curve in near the surface over a small depth λ_V, so as to fulfill the boundary condition (5). On inserting the second equation of state $\mathbf{J_s}(T,\boldsymbol{\omega},\mathbf{V_s})$ into Eqs. (2)–(4), explicit expressions for λ_V can be derived.[2,5] Currents $\mathbf{J_s}$ flowing in this surface layer to ensure the equilibrium of bent vortices are nothing but Meissner-like diamagnetic currents. The resulting *reversible* magnetic moment of the body is[2]

$$\boldsymbol{\mathcal{M}}=\int \tfrac{1}{2}\mathbf{r}\times\mathbf{J_s}d^3\mathbf{r}=\int -\boldsymbol{\varepsilon}d^3\mathbf{r}\approx-\boldsymbol{\varepsilon}_1 V, \qquad (6)$$

where V is the volume of the body, and $\boldsymbol{\varepsilon}_1(T,\boldsymbol{\omega}_1)$ is the bulk constant value of $\boldsymbol{\varepsilon}$. The second integral expression for $\boldsymbol{\mathcal{M}}$ in Eq. (6) is a strict consequence of Eqs. (4) and (5). It provides a formal interpretation of the vortex potential $\boldsymbol{\varepsilon}_1$ as an equivalent mean magnetization $-\boldsymbol{\mathcal{M}}/V$, and thereby a way to measure $\boldsymbol{\varepsilon}$ through a reversible magnetization curve.

In the MS model (Sec. II C), nondissipative transport currents and diamagnetic currents obey the same Eq. (4), so that the parameter $\boldsymbol{\varepsilon}(T,\boldsymbol{\omega},\mathbf{V_s})$ also governs amplitudes of the critical-current densities K_c (given a state of the surface). For a given material, at a given temperature, $\boldsymbol{\varepsilon}$ essentially depends of the vortex field $\boldsymbol{\omega}$. As discussed elsewhere,[2,5,9] the $\mathbf{V_s}$ dependence of $\boldsymbol{\varepsilon}$ may be ignored in most practical cases, so that the local value of $\boldsymbol{\varepsilon}$ at any point of a distorted lattice will be approximated by that of a uniform lattice of the same density and orientation. Note that, according to the form (1) of the thermodynamic identity, $\boldsymbol{\varepsilon}$ is not directly dependent on $\mathbf{B}$. We stress that $-\boldsymbol{\varepsilon}$ does not have the primary physical meaning of a local magnetization $\mathbf{M}$. As discussed in Ref. 2, the introduction of local fields $\mathbf{M}$ and $\mathbf{H}$ in the mixed state, even as substituting notations for $-\boldsymbol{\varepsilon}$ and $\mathbf{B}/\mu_0+\boldsymbol{\varepsilon}$, is unnecessary and misleading. As explained below, supercurrents $\mathbf{J_s}=-$curl $\boldsymbol{\varepsilon}$ may contribute to transport currents, contrary to equivalent magnetization currents $\mathbf{J_M}$ in a magnetic material, which are defined as curl $\mathbf{M}$. Also, we can no longer identify curl $\mathbf{H}$ as the transport current.[2]

B. The vortex potential of an uniaxial crystal

In the phenomenological GL theory, a material is characterized (at a given temperature) by two parameters, say, the GL parameter κ and the thermodynamic critical field B_c, and then, when dealing with an anisotropic crystal, by the principal values m_1, m_2, and m_3, of the reduced mass tensor $\mathbf{m}$ (defined so that $m_1m_2m_3=1$, and $m_{ik}=\delta_{ik}$ in the isotropic case).[10]

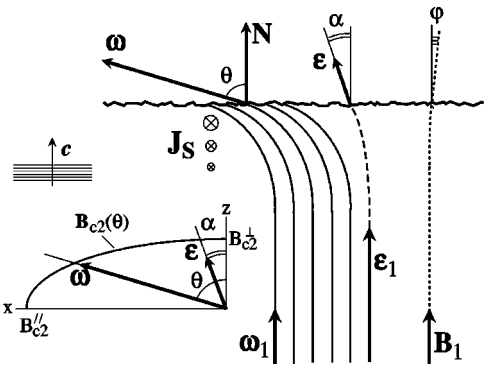

FIG. 1. Schematic of a possible equilibrium configuration of the vortex array near an *ab* face of an uniaxial crystal, immersed in normal field $\mathbf{B}_0$. Owing to surface irregularities on the scale of the vortex spacing, many such configurations may arise near the surface. Vortex distortions take place over a small healing depth $\lambda_V \leqslant \lambda_{ab}$, while vortices remain straight and uniformly distributed in the bulk. The vortex field $\boldsymbol{\omega}$ represents both the vortex density ω/φ_0 and direction of vortex lines. The vortex potential $\boldsymbol{\varepsilon}(\boldsymbol{\omega})$, defined in Sec. II A, is the local thermodynamic parameter that governs the existence of macroscopic currents $\mathbf{J_s}$. When $\boldsymbol{\omega}$ is inclined to the c axis by an angle θ, $\boldsymbol{\varepsilon}$ makes a smaller angle α with the c axis. The left inset shows the θ dependence of the upper critical field. If vortices are bent in the xz planes as shown in this figure, currents $\mathbf{J_s}=-$curl $\boldsymbol{\varepsilon}$, ensuring vortex equilibrium flow systematically in the y direction. These supercurrents may appear on the scale of the sample either as nondissipative transport currents or hysteretic diamagnetic currents. Note that vortex bending is of relatively low cost in free energy, as long as the magnetic field itself is not very distorted. In the perturbed layer, magnetic-field lines are not vortex lines, and they are slightly deviated in the opposite direction at angles $\varphi\sim\mu_0K/B_0\sim10^{-3}$.

Here we consider only layered uniaxial crystals, like $NbSe_2$, for which $m_1=m_2<m_3$, where m_3 is the principal value of $\mathbf{m}$ in the direction z of the c axis. Thus the anisotropy is described by one parameter, for instance, the *anisotropy factor*:

$$\gamma=(m_3/m_1)^{1/2} \quad (m_1=m_2=\gamma^{-2/3},\ m_3=\gamma^{4/3}). \qquad (7)$$

From theoretical calculations of the reversible equivalent magnetization,[10,11] we infer that $\boldsymbol{\varepsilon}$ lies along the vector $\mathbf{m}\cdot\boldsymbol{\nu}$ (or $\varepsilon_i=m_{ik}\nu_k$).[10,11] More explicitly, if vortices are inclined to the z or c axis by an angle θ, say, in the xz planes (see Fig. 1), $\boldsymbol{\varepsilon}$ also lies in the xz planes but makes a smaller angle α with the c axis, with θ and α being simply related by

$$\tan\theta=\gamma^2\tan\alpha. \qquad (8)$$

Equation (8) states that $\boldsymbol{\varepsilon}$ tends to keep aligned with the c axis, or at least lags considerably, when θ is increased. Taking $\gamma=3$, as corresponds to $NbSe_2$, $\alpha=20°$ when θ has exceeded 70°. Stated in another way, vortex currents $\mathbf{j_s}$, which flow in planes normal to $\boldsymbol{\varepsilon}$, [10,11] tend to stay in the *ab* planes when vortices are inclined to the c axis.

Again, the MS boundary condition (5) is consistent with the GL boundary condition for the order parameter. In an anisotropic crystal, the latter reads

$$\mu_{ik}\frac{\partial \rho}{\partial x_i}n_k = 0, \tag{9}$$

reducing to $\partial\rho/\partial n = 0$ in the isotropic case. Here $\mu_{ik} = m_{ik}^{-1}$ is the inverse mass tensor. Equation (9) requires that vortex lines enter the sample along the direction $\mu_{ik}n_k$, or equivalently, that the vector $m_{ik}\nu_k$ must be normal to the surface. That is just what is required by the condition (5).

The amplitude ε of the vortex potential decreases when the vortex density $\boldsymbol{\omega}$ is increased, and $\boldsymbol{\varepsilon}$ vanishes when $\omega = B_{c2}(\theta)$, an upper critical field depending on the vortex orientation as (Fig. 1):

$$\frac{B_{c2}(\theta)}{B_c\sqrt{2}} = \tilde{\kappa}(\theta) = \kappa_\perp[\gamma^{-2}\sin^2\theta + \cos^2\theta]^{-1/2}, \tag{10}$$

where $\kappa_\perp = \kappa(0) = \kappa m_1$, so that $\kappa_\parallel = \kappa(\pi/2) = \gamma\kappa_\perp$. The anisotropy factor is currently estimated from the upper critical-fields ratio $B_{c2}(\pi/2)/B_{c2}(0)$.

Near B_{c2}, the components of $\boldsymbol{\varepsilon}$ decrease linearly as $B_{c2} - \omega$. For $\boldsymbol{\omega}(\omega\sin\theta, 0, \omega\cos\theta)$ we have[10]

$$\boldsymbol{\varepsilon}_x = \frac{B_{c2}(\theta) - \omega}{2\mu_0\beta_A}\frac{\sin\theta}{\kappa_\parallel^2}, \tag{11}$$

$$\boldsymbol{\varepsilon}_z = \frac{B_{c2}(\theta) - \omega}{2\mu_0\beta_A}\frac{\cos\theta}{\kappa_\perp^2}, \tag{12}$$

where $\beta_A = 1.16$ for a triangular lattice. In Eqs. (11) and (12) we have ignored terms smaller than unity in the denominator, which can be fully neglected with respect to the quantity $2\kappa^2\beta_A$ when $\kappa \gg 1$. The above expressions of ε_x and ε_z have been derived under the assumption that $B_{c2} - \omega \ll B_{c2}$.[10] Their range of validity, however, is much larger than expected. Following a numerical procedure proposed by Brandt,[12] a precise solution of the GL equations can be computed for a regular vortex lattice, *arbitrary fields* $\omega = B$, and vortex orientation. In this way, we have calculated the constitutive relations $\varepsilon_x(\omega)$ and $\varepsilon_z(\omega)$ for several values of θ, in $NbSe_2$ at 4.2 K ($\kappa_\perp = 20$, $\gamma = 3$; see, for instance, Fig. 2). It turns out that expressions (11) and (12) may be used down to $\omega \sim 0.3B_{c2}$ with an accuracy better than 5%.

As expressions (11) and (12) have been established for a uniform lattice where $\boldsymbol{\omega} = \mathbf{B}$, they are usually expressed as functions of $B_{c2} - B$, instead of $B_{c2} - \omega$. Moreover, by virtue of Eq. (6), $-\boldsymbol{\varepsilon}_1 = -\boldsymbol{\varepsilon}(\boldsymbol{\omega}_1 = \mathbf{B}_1)$ is directly written as giving the equivalent reversible magnetization $\mathbf{M} = \boldsymbol{\mathcal{M}}/V$ of any simple shaped body as a function of the *internal field* $\mathbf{B}_1 = \boldsymbol{\omega}_1$. Nevertheless, that is a restricted physical meaning of $\boldsymbol{\varepsilon}$. As we will discuss further below, we shall have to estimate nondissipative currents, such as given by Eq. (4), at points where the vortex field $\boldsymbol{\omega}$ of a distorted array may be very different from $\mathbf{B}$: there, the local vortex potential $\boldsymbol{\varepsilon}$ must be expressed as a function of $\boldsymbol{\omega}$ and not $\mathbf{B}$. Thus, the "vortex density" $\boldsymbol{\omega}$ may well reach the critical value B_{c2}, while the line tension ε has fallen to zero, even though the local magnetic field B itself is far below B_{c2}. Notwithstanding the expression "critical field" for B_c or B_{c2}, neither the local condition $B = B_c$ or B_{c2}, in a type-I or -II sample, nor the condition $B_0 = B_c$ or B_{c2} for the applied field, implies a transition to the normal state. We known that thin type-I films remain superconducting in parallel fields much larger than B_c. In the present case, as explained in Sec. II C, a normal layer may arise at a rough surface in normal fields $B_0 < B_{c2\perp}$.

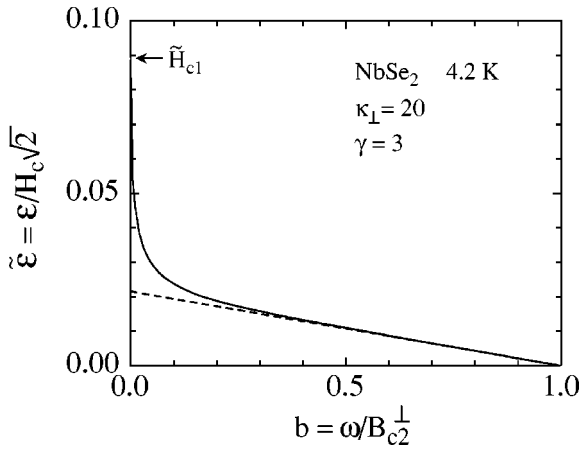

FIG. 2. The vortex potential ε of $NbSe_2$ (at 4.2 K) as a function of the vortex density ω, when the vortices are parallel to the c axis (θ, $\alpha = 0$; triangular lattice). The full line results from a numerical calculation of an exact solution of the GL equations. The dashed line is the linear approximation such as given by Eq. (12) with $\theta = 0$; in reduced units $\tilde{\varepsilon} = \tilde{\varepsilon}_z = (1-b)/2\beta_A\kappa_\perp$. Replacing ε by $-M$, and ω by B_0, this curve can be interpreted, more familiarly, as the reversible magnetization of a slab in normal field. However, it must be borne in mind that $-\boldsymbol{\varepsilon}$ does not have the primary physical meaning of a local magnetization.

C. Rough surfaces and nondissipative transport currents

The best samples are hardly free from surface irregularities. If the surface is rough on a scale comparable to or smaller than the vortex spacing, $\mathbf{n}$ is a highly variable vector, and, as pointed out above, the boundary condition (5) does not make sense in a continuum theory of the mixed state. Nevertheless, the set of continuum Eqs. (2)–(4) can be maintained, while assuming ideal smoothed surfaces, provided that the condition (5) is released. MS theory suggested to replace it by an inequality similar to a friction angle condition in mechanics:

$$|\hat{\boldsymbol{\varepsilon}} \times \mathbf{N}| < \sin\alpha_m, \tag{13}$$

where $\hat{\boldsymbol{\varepsilon}} = \boldsymbol{\varepsilon}/\varepsilon$ is a unit vector, and $\mathbf{N}$ now stands for the normal unit to the idealized mean surface. The physical meaning of Eq. (13) is clear. Consider, for example, the isotropic case where $\hat{\boldsymbol{\varepsilon}} = \boldsymbol{\nu}$: the vortex array may undergo a collective (macroscopic) bending near the sample surface so as to be inclined by an angle α to the mean normal $\mathbf{N}$. If α is not too large, each vortex line, at the cost of very small

displacements, may still terminate normal to the actual irregular surface as required by the GL boundary condition.

Equations (2)–(4), completed by condition (13), lead to an infinity of nondissipative metastable solutions. The magnetic moment of a body may strongly differ from the ideal value (6). Not only may diamagnetic currents change, causing hysteresis, but also nondissipative transport currents possibly occur. All these currents obey the same equations, and, therefore, they flow near the surface over the same depth λ_V.

Now, we confine ourselves to the standard geometry investigated in Sec. III. A slab (thickness $\Delta z = t$, width $\Delta x = W$) is immersed in a normal applied field $\mathbf{B}_0(0,0,B_0)$. The slab is an uniaxial single crystal, the thickness of which is perpendicular to the *ab* planes (*xy* planes). Vortex lines are regularly distributed in the bulk with a vortex density $\boldsymbol{\omega}_1 = \mathbf{B}_1$, the internal magnetic field (Fig. 1). Magnetizing effects are negligible so that $\mathbf{B}_1 = \mathbf{B}_0$. The bulk vortex potential $\boldsymbol{\varepsilon}_1(0,0,\varepsilon_1)$ is a decreasing function of the *reduced field*,

$$b = \frac{\omega_1}{B_{c2}^{\perp}} = \frac{B_0}{B_{c2}^{\perp}}, \tag{14}$$

as shown in Fig. 2.

Whereas the vortex density and orientation have uniform and well-determined values in the bulk, undetermined static distortions of the vortex array may settle over a depth λ_V from the surface. Suppose, for example, that vortices bend uniformly in the *xz* planes as sketched in Fig. 1, and intersect the (mean) surface with an angle of incidence θ. As stated by Eq. (8), $\boldsymbol{\varepsilon}$ makes a smaller angle $\alpha(\theta)$ with the normal $\mathbf{N}$. If $\alpha(\theta) < \alpha_m$, the vortex lines may fit the rough surface on a ''microscopic'' scale. According to Eq. (4), the currents $\mathbf{J_s}$ that balance this vortex bending must flow in the *y* direction.

It should be emphasized that, in such a distorted layer, vortex lines and magnetic-field lines bend in opposite directions (Fig. 1). Otherwise, the Lorentz force and the restoring force would act in the same direction and could not counterbalance each other. Therefore, this kind of equilibrium could not be conceived, as long as the vortex lines and magnetic-field lines were confused. The equilibrium of bent vortices immersed in diamagnetic currents near the faces of a (perfect) slab inclined to the applied field is quite similar. With this difference, in the latter case, currents on both faces of the slab are in opposite directions and cancel out. Instead, currents on both faces of a rough slab may flow in the same direction, giving rise to a net transport current.

On integrating J_{sy} over their penetration depth, we find the surface current density

$$K_y = -\varepsilon_x(\boldsymbol{\omega}), \tag{15}$$

where $\boldsymbol{\omega}$ is the vortex field *at the surface*. In magnitude (A/m),

$$K = |\varepsilon_x(\omega,\theta)| = \varepsilon(\omega,\theta)\sin\alpha. \tag{16}$$

The vortex density ω at the surface is larger than the bulk density ω_1, in accordance with the law of conservation of the number of vortex lines (or div $\boldsymbol{\omega} = 0$). As easily seen,

$$\omega = \frac{\omega_1}{\cos\theta} = \frac{bB_{c2}^{\perp}}{\cos\theta}. \tag{17}$$

Let us return to the *isotropic* case momentarily. As $\theta = \alpha$ seldom exceeds 20°, we may disregard, as a first approximation, the variation of the vortex density near the surface. Thus, assuming $\omega = \omega_1$ and $\varepsilon = \varepsilon_1$, Eq. (17) reduces to $K = \varepsilon_1 \sin\alpha$. To a maximum, $K = K_c$, the MS critical-current density is

$$K_c = \varepsilon_1 \sin\alpha_m, \quad \text{(isotropic slab)}. \tag{18}$$

Collecting I_c data in slabs or foils of conventional *isotropic* and soft materials (lead alloys and pure metals) and letting $K_c = I_c/2W$, Mathieu *et al.* extracted empirical values of α_m within the range 0.5°–25°.[1,2,13] Note that $\sin\alpha_m$, although it is an adjustable parameter, was always found to be reasonably less than the unity, as it should be. Furthermore, the temperature dependence of ε_1 well accounts for the T dependence of critical currents.[13] The limiting angle α_m is a statistical and geometrical property of a rough surface, for a given density ($n_1 = \omega_1/\varphi_0$) of intersecting points between vortex lines and the surface. Clearly α_m increases with increasing roughness. It also increases when the vortex density n_1 is decreased at low fields. In the absence of any treatment to make the surface very smooth or very rugged, α_m is typically of the order of a few degrees. In this case, $\omega = \omega_1$ within better than 1%, and the approximated formula (18) is quite justified in the whole field range.

Conclusions are quite different for an *anisotropic* material. While α_m should sweep the same range of values, we can no longer ignore the increase in the vortex density accompanying the strong vortex bending. To be explicit, let $\gamma = 3$ ($NbSe_2$), $B_0 = \omega_1 = 0.7B_{c2}^{\perp}$ ($b = 0.7$), and suppose that $\alpha = 20°$ as allowed by an enhanced roughness. According to Eqs. (8) and (10), vortices intersect the mean surface with an angle of incidence of $\theta = 73°$, for which the upper critical field $B_{c2}(\theta = 73°)$ is larger than $B_{c2}^{\perp}$ by a factor of 2.3. Now, as required by Eq. (17), the vortex density ω at the surface should be as large as $3.4\omega_1 = 2.4B_{c2}^{\perp} > B_{c2}(\theta)$. This means that for $b = 0.7$, ε and the current density $K(\alpha)$ have fallen to zero before 20° (as shown in Fig. 3), and $K(\alpha)$ is a *maximum* at some intermediate value α_0. As pointed out above, what becomes critical here is the vortex density, whereas the magnetic field remains practically uniform throughout the slab including where the vortex lattice is distorted.

Making use of Eqs. (8), (10), and (11), and substituting α and the reduced field b as independent variables for ω and θ in Eq. (16), we obtain

$$K(\alpha) = \frac{B_{c2}^{\perp}}{2\mu_0\beta_A\kappa_{\perp}^2}\tan\alpha\left[(1+\gamma^2\tan^2\alpha)^{-1/2} - b\right]. \tag{19}$$

At a given applied field b, the nondissipative current density K is a maximum for some angle α_0:

$$\alpha_0 = \tan^{-1}\left(\gamma^{-1}\sqrt{b^{-2/3}-1}\right). \tag{20}$$

On substituting α_0 for α in Eq. (19), we find

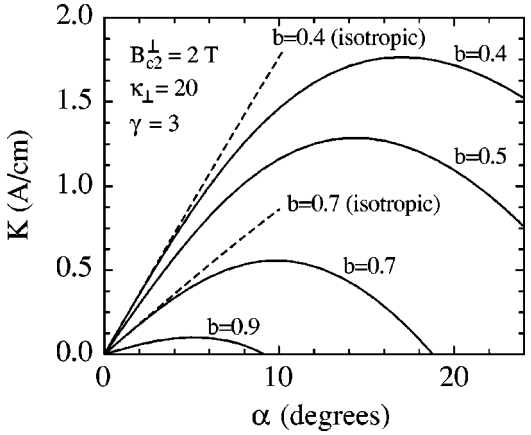

FIG. 3. An equilibrium configuration of the vortex array, like that sketched in Fig. 1, where vortices are bent in the *xz* planes, is kept balanced by supercurrents flowing in the *y* direction. For a given value of the bulk vortex density $\omega_1 = B_0 = bB_{c2}^{\perp}$, such a configuration is uniquely determined by the angle α, at the surface, between the vector $\boldsymbol{\varepsilon}$ and the normal to the mean smoothed surface. The total surface current density K, obtained by integrating J_{sy} over z, is plotted in this figure as a function of α, for a few values of the reduced field b. Full lines are calculated from Eq. (19) by taking $\gamma = 3$, $\kappa^{\perp} = 20$, and $B_{c2}^{\perp} = 2$ T, i.e., the relevant parameters of $NbSe_2$ at 4.2 K. Dashed lines are obtained by merely substituting $\gamma = 1$ for $\gamma = 3$. The maximum of $K(\alpha)$ for relatively low values of α is a characteristic feature of the anisotropy. This maximum explains that critical currents become saturated when the surface roughness is increased.

$$K_0(b) = K(b, \alpha_0) = \frac{B_{c2}^{\perp}}{2\mu_0 \beta_A \gamma \kappa_{\perp}^2} (1 - b^{2/3})^{3/2}. \qquad (21)$$

Equation (21) represents an upper bound for the nondissipative MS current for a given applied field. *As far as vortices can fit the rough surface freely*, and the surface is rough enough so that $\alpha_m > \alpha_0$, the expected critical-current density is $K_c = K_0$. If $\alpha_m < \alpha_0$, $K_c = K(\alpha_m)$ such as given by Eq. (19), and $K_c < K_0$.

As a conclusion, we predict that critical currents of an uniaxial slab become saturated, when the roughness of the faces is increased. Moreover, the saturation critical current is expressible in terms of the fundamental parameters of the material [Eq. (21)], without any adjustable parameter.

In theory, the above equations hold in the isotropic case. However, the condition for observing the saturation $\alpha_m > \alpha_0$ $(b, \gamma = 1)$ cannot be achieved except in a too restricted field range near B_{c2}. For example, taking $b = 0.5$ in Eq. (20), we obtain $\alpha_0 = 14°$ for $\gamma = 3$, but $\alpha_0 = 37°$ for $\gamma = 1$. The former is readily accessible, but the latter exceeds the limiting angles of the roughest surfaces.

TABLE I. The residual resistivity ratio and dimensions of the $NbSe_2$ slabs referred to in Figs. 4 and 5. Samples S5a and S5b have been detached from the same ampoule.

	RRR	Width (mm)	Thickness (mm)	Length (mm)
S4	54	2.2	0.12	8.1
S5a	44	1.5	0.17	11.5
S5b		1.5	0.14	5.4

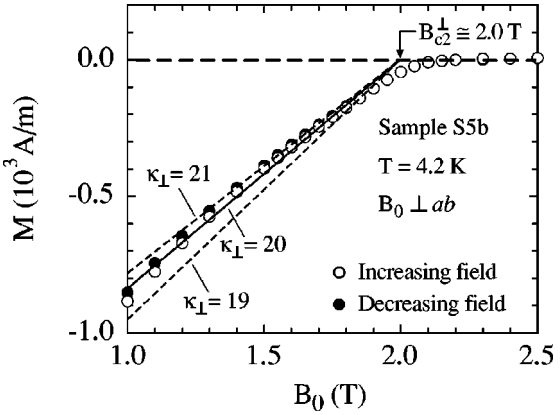

FIG. 4. The magnetization of the sample S5b in normal field. Open and full circles correspond to increasing and decreasing fields, respectively. These data have been corrected for a small paramagnetic contribution mainly due to the sample holder. Straight lines are fits to the linear expression (12), letting $M = -\varepsilon_z(\theta = 0, \omega = B_0)$. So we obtain $\kappa_{\perp} = 20 \pm 1$, and $B_{c2}^{\perp} = 2.0 \pm 0.1$ T. The absence of a "peak effect" in magnetization curves made the fit easier.

III. EXPERIMENTAL RESULTS

Single crystals of $NbSe_2$ have been grown from prereacted polycrystalline powder by a standard method of chemical vapor transport using iodine as a gas vector in a three-zone thermal profile.[14,15] The crystal structure was confirmed to be in the $2H$ phase by x-ray diffraction. Crystals obtained by this method appeared in the form of thin faceted platelets with a mirrorlike surface perpendicular to the *c* axis. Rectangular slabs were cut out of large-sized crystals (see Table I). Transition temperatures, as determined by low-field magnetic susceptibility, were close to 7.15 K. The residual resistivity ratio (RRR) defined as the ratio $R(300\,\mathrm{K})/R(7.5\,\mathrm{K})$ is around 40–50. These values of RRR and T_c agree with those previously published,[14,15] and attest to the good quality of our crystals.

All measurements reported in this paper were carried out at the temperature 4.2 K. Experimental data in Figs. 4 and 5 refer to the three samples described in Table I. Critical currents I_c were measured in perpendicular field $\mathbf{B}_0 \perp ab$, in the range $0.2 < b < 1$. We used a standard four-lead arrangement, copper wires being attached to the crystal with silver paste. Then $K_c = I_c/2W$ is compared with theory (Fig. 5).

The magnetization of some of the slabs was studied, in perpendicular and parallel fields, with a commercial superconducting quantum interference magnetometer (Quantum Design, model MPMS). From the reversible part of the magnetization curves $M_{\perp}(B_0)$ and $M_{\parallel}(B_0)$, we could extract the three parameters involved in equations of Sec. II, which characterize the uniaxial crystal, namely, $B_{c2}^{\perp}$, $\kappa_{\perp}$, and γ. A fit of the linear part of $M_{\perp}(B_0)$ to Eq. (12), assuming $M_{\perp} = -\varepsilon_z(\omega = B_0, \theta = 0)$, gives $B_{c2}^{\perp} = 2.0$ T and $\kappa_{\perp} = 20$ (Fig. 4). Note that the demagnetizing effects are completely neg-

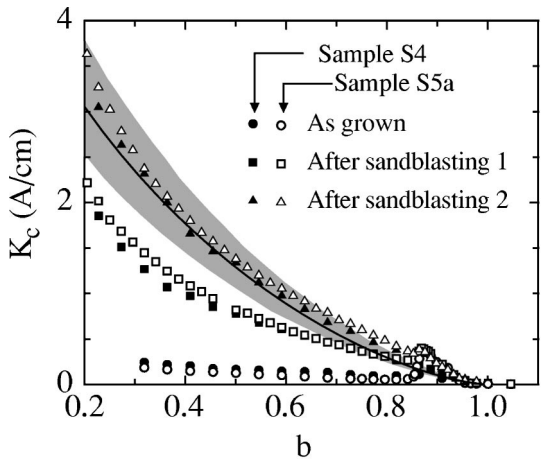

FIG. 5. The surface critical-current density, defined as $K_c = I_c/2W$, as a function of the reduced magnetic field b, before and after two successive sandblasting processes. In the first process, the nozzle-sample distance d was 8 cm, and the time of exposure $\tau = 1$ min. In the second process, $d = 4$ cm, and $\tau = 20$ s. The full line $K_0(b)$ is the upper bound of $K_c(b)$ such as predicted by the theory of Sec. II C. Here $K_0(b)$ has been calculated by letting $\gamma = 3$, $\kappa_\perp = 20$, and $B_{c2}^\perp = 2$ T in Eq. (21). The dashed area stands for the experimental uncertainty in these parameters (mainly in $\kappa_\perp$).

ligible. The demagnetizing factor D of a slab such as the sample S5b (Table I) is about 0.9, and in writing $M_\perp = -\varepsilon$ ($\omega = B_0$) we disregard a small correcting term of the order $(1-D)/2\kappa_\perp^2\beta_A \approx 10^{-4}$. Finally, the anisotropy factor $\gamma = 3$ was obtained as the ratio of the upper critical fields $B_{c2}^\parallel$ and $B_{c2}^\perp$.

As-grown crystals have very low critical currents (lower curve in Fig. 5). When interpreted as MS surface currents through Eq. (19), they correspond to a limiting angle as low as $\alpha_m \sim 1°$. As explained in Sec. II, such values of α_m have been found to be typical of the best polished surfaces in a variety of conventional materials. In order to appreciate the effect of increasing roughness on the critical current, both faces of the slabs were roughened by moderate and gradual sandblasting. For this purpose, we used a commercial system (Sandmaster GF 1-93) operated with 9-μm alumina powder, and low gas pressure (1.5 bar). We still had to adjust the distance d between the nozzle and the sample, and the time τ of exposure; typically, $d \sim 5-10$ cm, and $\tau \lesssim 1$ min. Sandblasting must be gentle enough to preserve the sample thickness, while yet achieving large roughness angles $\alpha_m \gtrsim 20°$. The state of the sandblasted surface was controlled by atomic force microscopy. Maximum rms standard deviations of the surface profile were about 50–60 nm.

The fact that the critical current I_c of a slab increases when its surface is sandblasted is in itself not surprising. Independently of any theoretical interpretation, the roughness dependence of critical currents becomes more significant and simply stated, when expressed in terms of the surface critical-current density defined as $K_c = I_c/2W$. First, slabs of different dimensions, subject to the same surface treatment by sandblasting, acquire the same critical-current density K_c. Then, while increasing roughness, K_c seems to reach a reproducible saturation value $K_0(b)$. Figure 5 shows how this saturation value is attained after two successive sandblasting processes. If we confine ourselves to these qualitative features, however, we cannot decide on any particular mechanism, even though surface defects are clearly involved. Nor do we know whether $K_0(b)$ represents some practical limiting value, or a fundamental upper bound of $K_c(b)$.

The striking and conclusive result here, is that the observed saturation current $K_0(b)$ is close to the theoretical maximum of the MS nondissipative current in an uniaxial crystal, also denoted as $K_0(b)$ in Sec. II [Eq. (21) and the full line in Fig. 5]. The quantitative agreement between theory and experiment is as satisfactory as we could hope for because of the experimental errors and underlying approximations: (i) The usual accuracy in measuring I_c and W, (ii) the uncertainty in the fundamental parameters, in particular $\kappa_\perp$ ($\kappa_\perp = 20 \pm 1$; see Figs. 4 and 5), and (iii) the use of approximated expressions for ε. Also by taking $\beta_A = 1.16$, we have deliberately ignored a small increase in the Abrikosov parameter β_A associated with the deformation of the basic cell of the vortex lattice in the vicinity of the surface. (iv) In addition, the approximation inherent in a continuum description of the vortex state, especially as the depth λ_V, is not much larger than the maximum standard deviation of the surface profile. These remarks should not obscure the main outcome of this work: we are able to predict the absolute value of the critical currents of a rough crystal of $NbSe_2$, without any adjustable parameter.

IV. DISCUSSION

The fitting of the vortex lattice to the disordered boundary conditions of a rough surface offers the possibility of quasisuperficial nondissipative transport currents. We stress again that this mechanism is not one of vortex pinning in the proper sense. Measurements of critical currents in $NbSe_2$ uniaxial crystals, at intermediate and high fields, provide strong support for the correctness of the MS interpretation, and reinforce the idea that MS currents account for the whole critical current in many soft samples. However, we cannot exclude that, in some samples, vortex pinning or some other mechanism comes into play, giving rise to an additional source of critical currents. In any case, the contribution of the MS currents should be taken into account.

In this connection, let us refer to an incidental observation. While working out the growth method, the analysis of the first crystals obtained revealed a lack of stoichiometry, and the presence of crystallized phases of iodoselenides. At the same time, these samples exhibited a strong ''peak effect'' near H_{c2} ($0.8 \lesssim b < 1$), including those in the magnetization curves. In the $K_c(b)$ curves, the peak effect appeared as a superimposed contribution insensitive to an increase in the surface roughness. These chemical defects were removed by a more careful preparation of the prereacted powder; correlatively, peak effects disappear, except perhaps for a small residual effect in the $K_c(b)$ curve (see Fig. 5), which does not affect our conclusions. We suggest that the enhancement of critical currents in the ''peak effect'' might be due this

time to a very strong pinning effect, which becomes effective near H_{c2}.

Theoretical considerations of Sec. II should apply to YBaCuO. The order of magnitude of critical currents in the low-field limit, as quoted in Sec. I, are well explained by the MS model.[16] Clearly, however, the saturation effect is not observed. In particular, critical currents vanish in the so-called vortex liquid phase above the irreversibility line. Now, as pointed out in Sec. II A, the MS model works for a vortex liquid as well. On account of the usual roughness of epitactic YBaCuO,[7] critical current ought to exist up to H_{c2}. The question thus arises as to why the $NbSe_2$ scenario is not recurring in YBaCuO. In Sec. II C, an essential condition for observing the saturation effect has been stated: vortices must fit the surface *freely*, in order to achieve the configuration that maximizes the current density. We think that this condition possibly fails in YBaCuO, for reasons that need to be elucidated. In an attempt to explain the irreversibility line in the frame of the MS model, Simon, Plaçais, and Mathieu made the assumption that collective distortions of the vortex array, randomly directed, preexist along the surface.[16] Such distortions should be hysteretic or metastable states depending on the past history of the sample. They prevent the saturation current from being observed, while accounting for the vanishing of the critical currents at high fields.[16] The existence of frozen deformations implies free-energy barriers. As the vortex line tension $\varepsilon\varphi_0$ falls off for strong bending, it is plausible that strong deformations be paradoxically of less free energy than weak deformations, giving rise to free-energy barriers. If we were able to prepare a vortex state, free from large surface distortions, in the region of the phase diagram usually assigned to the vortex liquid, we should retrieve a nonzero critical current at the first onset of a dc current. An experiment is planned to verify this assumption.

ACKNOWLEDGMENT

J.M. acknowledges a grant from the Fundación Caixa Galicia.

*Present address: LBTS Departamento de Física de Materia Condensada, Universidade de Santiago de Compostela, E15782, Spain [unit associated with the Consejo Superior de Investigaciones Científicas (Spain)].

[1] P. Mathieu and Y. Simon, Europhys. Lett. **5**, 67 (1988).
[2] T. Hocquet, P. Mathieu, and Y. Simon, Phys. Rev. B **46**, 1061 (1992).
[3] B. Plaçais, P. Mathieu, and Y. Simon, Phys. Rev. Lett. **70**, 1521 (1993).
[4] N. Lutke-Entrup, B. Plaçais, P. Mathieu, and Y. Simon, Phys. Rev. Lett. **79**, 2538 (1997); Physica B **255**, 75 (1998).
[5] B. Plaçais, P. Mathieu, Y. Simon, E. B. Sonin, and K. B. Traito, Phys. Rev. B **54**, 13 083 (1996).
[6] W. C. H. Joiner and G. E. Kuhl, Phys. Rev. **163**, 362 (1967).
[7] Ch. Joos, A. Forkl, R. Warthmann, H. U. Habermaier, B. Leibold, and H. Kronmüller, Physica C **266**, 235 (1996).
[8] E. Sheriff, R. Prozorov, Y. Yeshurun, A. Shaulov, G. Koren, and C. Chabaud-Villard, J. Appl. Phys. **82**, 4417 (1997).
[9] B. Plaçais, Ph.D. thesis, Université Pierre et Marie Curie, 1990.
[10] V. G. Kogan and J. R. Clem, Phys. Rev. B **24**, 2497 (1981).
[11] L. J. Campbell, M. Doria, and V. G. Kogan, Phys. Rev. B **38**, 2439 (1988).
[12] E. H. Brandt, Phys. Rev. B **78**, 2208 (1997).
[13] B. Plaçais, P. Mathieu, and Y. Simon, Solid State Commun. **71**, 177 (1989).
[14] G. Vacquier and A. Casalot, J. Cryst. Growth **130**, 259 (1993).
[15] C. S. Oglesby, E. Bucher, C. Kloc, and H. Kohl, J. Cryst. Growth **137**, 289 (1994).
[16] Y. Simon, B. Plaçais, and P. Mathieu, Phys. Rev. B **50**, R3503 (1994).